

Applications of Bio-Inspired Special Wettable Surfaces

Xi Yao, Yanlin Song,* and Lei Jiang*

In this review we focus on recent developments in applications of bio-inspired special wettable surfaces. We highlight surface materials that in recent years have shown to be the most promising in their respective fields for use in future applications. The selected topics are divided into three groups, applications of superhydrophobic surfaces, surfaces of patterned wettability and integrated multifunctional surfaces and devices. We will present how the bio-inspired wettability has been integrated into traditional materials or devices to improve their performances and to extend their practical applications by developing new functionalities.

1. Introduction

The ability to control a solid surface of specific wettability is of universal importance in academic sciences and industrial technologies. Among these, research on the topic of bio-inspired surfaces with special wettability is a large and growing field.^[1–9] Researchers from many fields, such as biology, physics, chemistry, material and engineering, have been attracted to this dynamic area where innovations and creations emerge every day.

Nature abounds with mysterious biological organisms that exhibit special surface wettability, such as the self-cleaning property of lotus leaves,^[10–14] the superior water-walking ability of water striders,^[15,16] the directional adhesion of butterfly wings,^[17] the antifogging functionality of mosquito eyes,^[18] the antireflection of superhydrophobic cicada wings,^[19] the water collection of the Namib Desert beetle and spider silk,^[20,21] the submarine self-cleaning ability of fish scale,^[22] and the use of plastron property for underwater breathing.^[23,24] Biomimetic research indicates that the cooperation of the unique structural design of these biological materials or organisms with intrinsic material properties play a crucial role to achieve the desired wettability and functionalities. On one hand, a lot of effort has been devoted to explore the structure–function relationship of different natural materials. New artificial materials or devices of special wettability are also functionalized by this strategy. On the other hand, it is the great potential in functional applications

presented by the improved performances of artificial materials that provides a direct impetus to push the field forward rationally. Although the practical application of nature-inspired surfaces is still limited, a lot of effort is gradually being accumulated, providing a great opportunity for the development of various laboratorial and industrial products. By searching in ISI Web of Science using the topic of “superhydrophobic or superhydrophobicity”, one can clearly observe an accelerated increase for the number of papers (Figure 1).

In this review, we focus on the recent developments in the practical applications and potential applications of bio-inspired special wettable surfaces. Our short review is not intended to be exhaustive in the vast body of the published literature. Rather, we want to highlight those materials that in our opinion represent the greatest advance in their respective fields in recent years, and which may be of significant importance for future applications. As shown in Figure 2, these aspects are divided to three groups: applications of superhydrophobic surfaces, surfaces of patterned wettability and integrated multifunctional surfaces and devices. We will present how the bio-inspired special wettability has been integrated into traditional materials or devices to improve their performances and to extend their practical applications by developing new functionalities. After the brief introduction, we summarize the applications of bio-inspired special wettability section by section. Finally, we briefly present our personal view of the remaining challenges for the future within this field of research.

2. Application of Superhydrophobic Surfaces

2.1. Functional Textiles of Special Wettability

Although the field of superhydrophobicity and the realization of surface micro- or nanostructure and wettability are attractive topics in recently years, to make surfaces water-repellent has been well-established in the textile industry since 1940s.^[25,26] As a famous example, the Wenzel and Cassie equations are both initialized from the consideration of the textile's wettability.^[27,28] Recent biological investigations deepen the understanding of the effect of nanostructure on the surface wettability, and advanced manufacture technique bring the textiles extra functionalities.

A general strategy to fabricate self-cleaning textiles is to modify the textile fibers with hydrophobic coatings to make them superhydrophobic. Among the various treating procedures, sol-gel process is an efficient approach to impart multifunctional properties to the treated samples.^[29–31] Gao

Dr. X. Yao, Prof. Y. Song, Prof. L. Jiang
Center of Molecular Sciences
Key Laboratory of Organic Solids
Institute of Chemistry
Chinese Academy of Sciences
Beijing 100190, P. R. China
E-mail: ylsong@iccas.ac.cn; Jianglei@iccas.ac.cn

DOI: 10.1002/adma.201002689

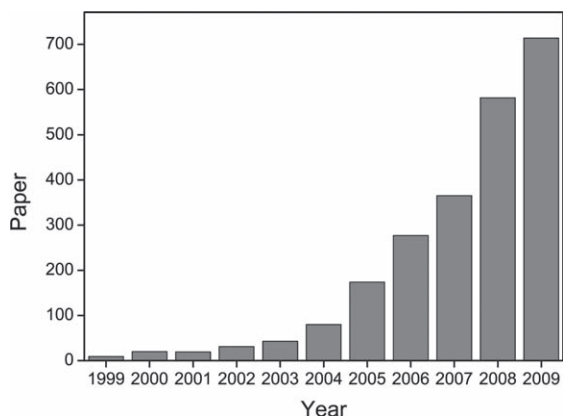


Figure 1. The statistics of the paper indexed in the ISI web of science by the topic of "superhydrophobic or superhydrophobicity".

and McCarthy reported a successful modification of two commercial polyester textiles with a simple water-repellent silicone coating procedure which patented in 1945.^[32] The two polyester textiles, one conventional polyester ^CPF and the other microfiber polyester fabrics ^HPF, are modified to achieve superhydrophobicity by dipping in a toluene solution of 4 wt% methylsilicone and dried at 100 °C for 1 h. Ming *et al.* has successfully obtained superhydrophobic cotton textiles by introducing silica micro/nanoparticles to the woven fiber network followed by surface modification.^[33,34] When the textiles of dual structures are modified with hydrophobic polydimethylsiloxane (PDMS), the hydrophilic cotton is turned to superhydrophobic, and it will also be superoleophobic after surface perfluorination. Besides the normal hydrophobic treatment, introducing functional materials can bring textiles more advantages. Orel and Simončič reported the preparation of multifunctional, water and oil repellent and antimicrobial finishes for cotton fabrics by a sol-gel process using a commercial fluoroalkyl water-born siloxane (FAS),

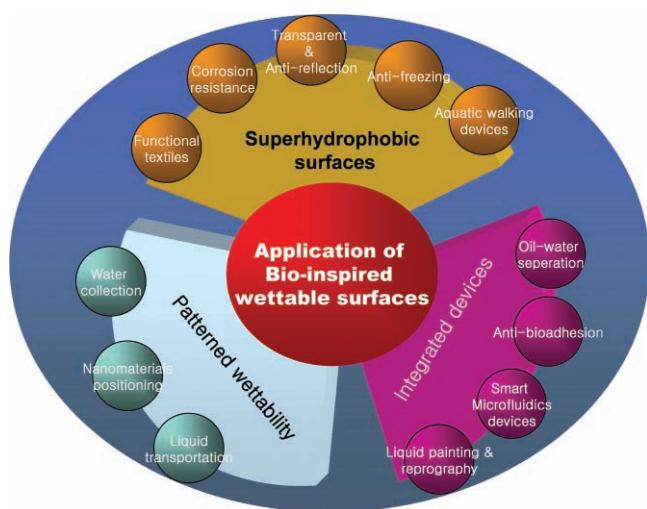


Figure 2. Applications of bio-inspired special wettability. The summarized topics include three areas, the surfaces of superhydrophobicity, surfaces of patterned wettability and integrated multifunctional surfaces and devices.



Lei Jiang is currently a professor at the Institute of Chemistry, Chinese Academy of Sciences (ICCAS), and Dean of the School of Chemistry and Environment, Beihang University. He received his B.Sc. degree (1987), M.Sc. degree (1990), and Ph.D. degree (1994) from Jilin University of China. He then worked as a postdoctoral fellow in Professor Akira Fujishima's group in Tokyo University. In 1996, he worked as a senior researcher in Kanagawa Academy of Sciences and Technology under Professor Kazuhito Hashimoto. He joined ICCAS as part of the Hundred Talents Program in 1999. In 2009, he was elected academician of the Chinese Academy of Sciences. His scientific interest is focused on bio-inspired surface and interfacial materials.

He then worked as a postdoctoral fellow in Professor Akira Fujishima's group in Tokyo University. In 1996, he worked as a senior researcher in Kanagawa Academy of Sciences and Technology under Professor Kazuhito Hashimoto. He joined ICCAS as part of the Hundred Talents Program in 1999. In 2009, he was elected academician of the Chinese Academy of Sciences. His scientific interest is focused on bio-inspired surface and interfacial materials.



Yanlin Song is a professor and Director of Laboratory of New Materials at ICCAS. He is also a board member of the Chinese Materials Research Society, an executive member of China Computer Industry Association, and deputy director of Chinese Society of Particology. He received his Ph.D. degree from the Department of Chemistry at Peking University in 1996. Between 1996 and 1998, he conducted research as a post-doctoral fellow in the Department of Chemistry of Tsinghua University. He then joined ICCAS in 1998. His research interests cover the areas of High density storage materials, smart photonic crystals and green printing plate technology.

He then joined ICCAS in 1998. His research interests cover the areas of High density storage materials, smart photonic crystals and green printing plate technology.



Xi Yao is currently a Ph.D. student at ICCAS. He received his B.Sc. degree in chemistry from Wuhan University, China in 2005. In 2005, he joined Prof. Lei Jiang's group at ICCAS. His current scientific interests are focused on pursuing the special wetting phenomena of biological organisms, particularly the water strider legs, understanding their structure-related unique surface physical and chemical properties, and fabricating bio-inspired intelligent materials.

His current scientific interests are focused on pursuing the special wetting phenomena of biological organisms, particularly the water strider legs, understanding their structure-related unique surface physical and chemical properties, and fabricating bio-inspired intelligent materials.

silver nanoparticles and a reactive organic-inorganic binder.^[35] Besides the inherent antibacterial effect of silver nanoparticles embedded in finishes, the low surface energy of the oleophobic finished cotton (caused by FAS), is considered to prevent or at least hinder the adhesion of bacteria and their consequent growth and formation of a biofilm on the finished fabrics, providing a kind of 'passive antimicrobial activity' effect. They also reported the treatment of cotton fabrics by sol-gel hybrid of mixed PDMS and perfluorosilane.^[36] The finished textile exhibits superhydrophobicity and oleophobicity with enhanced washing fastness, providing a long lasting passive antibacterial effect without the addition of any antibacterial agents. The high washing fastness of the treated finishes is due to not only the enrichment of the fluoro-content in the finishes, but also the surface mobility of the fluoroalkyl polyhedra silsesquioxane ousted from the coating interior during consecutive washings, which provides a highly regenerative oleophobic effect to the finished cotton fabrics.

The plasma technique is another excellent way to prepare water-repellent surfaces, by which surface roughness and low-surface-energy coatings can be anchored on the as-prepared material simultaneously.^[37–40] The plasma modification offers many advantages over the conventional chemical processes. The pollutants and the corresponding cost of effluent treatment can be efficiently reduced, resulting in a more economical and ecological process. Moreover, it can be developed in a wide pressure range, large reactor chamber and roller systems for large surface areas, which is available for industrial applications. The author's group developed a two-step procedure to obtain self-cleaning super-amphiphobic (superhydrophobic and superoleophobic) cashmere textiles by low temperature plasma treatment (Figure 3).^[41] Nanoscale roughness can be introduced on the texture surface after the plasma treatment. The further modification of fluorocarbons will largely decrease the surface energy of the textiles and thus makes the textiles water/oil-repellent. Moreover, the treatments will not change the original properties of the textiles, such as color, permeability, soft and flexibility.

Till now, many new commercial products consisting of durable self-cleaning textile fabrics have been designed. Still, challenges exist for the self-cleaning fabrics. The water-repellent textiles are expected to maintain their original external appearance after the surface treatments. They should exhibit appropriate softness and the hydrophobic coatings can present good durability for washing, sunlight, and high or low temperature exposure. Considering mass production in the textile industry, the procedure of cost-effective, eco-friendly will be appreciated.

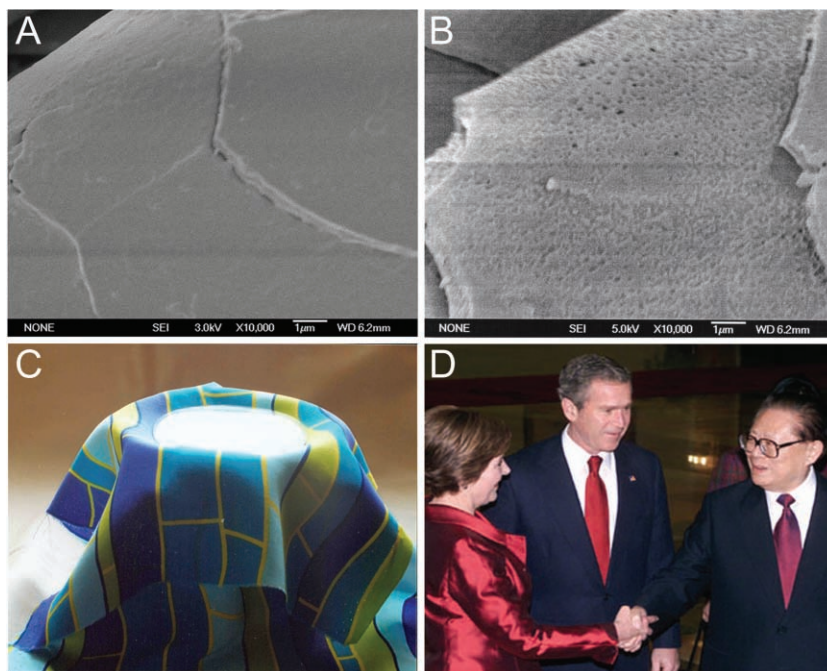


Figure 3. (A) The SEM image of the untreated cashmere textile; (B) Micro/nano Structure on cashmere after plasma treatment; (Unpublished data) (C) The product of super-amphiphobic textiles; (D) The self-cleaning nano-tie presented to former US President George Bush and Chinese President Jiang Zemin in 2002.^[41] Reprinted with permission.^[41] Copyright 2005 Nature Publishing Group.

2.2. Enhanced Corrosion Resistance

The oxidation and corrosion of metals in the humid atmosphere limit their application and bring huge waste and environmental contamination. Casting hydrophobic or superhydrophobic coatings on metal surfaces is a probable solution to these problems as the result of the intrinsic water-proof property of the coatings. It has been reported that self-assembled monolayers, such as alkyl silanes and thiols, hold promise as protective coatings because they can form thin closely packed barrier films on the coinage substrates.^[42–45]

Recently, researches show that treating metal or alloy surfaces to be superhydrophobic can improve the durability of the films for kinds of solvents and corrosive solution.^[46–49] Chemical bindings on metal surfaces can enhance the adhesion of the superhydrophobic coatings to the substrates, ensuring robust practical applicability. Hermelin *et al.* reported a one-step method of electrochemical depositing hydrophobic polypyrrole (PPy) coatings on zinc electrodes, in which 2 μm of PPy could be deposited in less than 3 s.^[50] The treated coatings show high hydrophobicity with contact angles around 125° as well as a highly increased barrier effect. The film shows improved anticorrosion property, where 1 μm of the film is equivalent to 1 μm of a zinc coating for preventing the corrosion of mild steel. Zhang *et al.* reported the fabrication of a ZnAl-LDH (Layered double hydroxides)-laurate (n-dodecanoate) film by anion exchange of laurate with a ZnAl-LDH-NO₃ film on a porous anodic alumina/aluminum (PAO/Al) substrates.^[51] The micro- and nanoscale hierarchical surface structures make the film

superhydrophobic, which provides long-term corrosion protection of the coated aluminum substrate and provides an effective barrier to aggressive species. The dc polarization measurements show that current density of the LDH-laurate film coating is as low as 10^{-8} A cm⁻², exhibiting an enhanced corrosion-resistant property far superior to the hydrophilic LDH-NO₃ film. Liu *et al.* reported the fabrication of the superhydrophobic surfaces on copper substrates, by immersing copper surfaces into n-tetradecanoic acid ethanol solution, which could remain intact in seawater for a month.^[52,53]

Making the metal surfaces superoleophobic is also important in corrosion inhibition. Jiang's group successfully achieved surface superoleophobicity on common engineering metals (zinc, aluminum, iron, and nickel) and their alloys (Zn-Fe alloy and brass) taking advantage of an electrochemical reaction in perfluorocarboxylic acid solutions.^[54,55] The moderate reactivity of the metals makes the surface reactions valid. Wu *et al.* fabricated a kind of multiple facet supported alumina nanowire forests by a high field anodization process.^[56] After modified with perfluorosilane, the surface exhibits super-repellency with low adhesion towards a broad range of liquids, such as hexadecane, silicone oil, liquid paraffin, crude oil etc.. Even the materials of low melting point such as solid paraffin and polyglycol upon melting can form globules and roll off the surface easily.

2.3. Transparent and Antireflective Coatings

Optical transparency or antireflective properties are basic requirements for many optical materials and devices, such as building windows, optical windows for electronic devices, eyeglasses, optical mirrors and lens. For most of them, the water repellent property or self-cleaning ability is also useful or even necessary. Thus, it is of great interest to integrate the superhydrophobicity with optical transparency or antireflective property within the same surface. The key for fabricating transparent or antireflective superhydrophobic surface is to optimize the surface roughness, since surface roughness usually enhances light scattering and reduces transparency.

Generally, for optical transparent surfaces, the roughness dimension should be lower than the wavelength of target light (380 nm ~ 760 nm for visible light), and is usually in the range of nanometer scale. Nakajima and co-workers reported serial works on the fabrication of inorganic transparent superhydrophobic films by introducing controllable nanometer thickness coatings with subsequently fluoroalkylsilane modification, which is in fact one of the basic strategies to fabricate transparent superhydrophobic coatings.^[57-59] A sublimable compound, aluminum acetylacetonate (Al(C₅H₇O₂)₃) is firstly developed to process films with suitable levels of roughness. They found that to obtain both the surface superhydrophobicity and transparency, the roughness of the prepared surfaces should be precisely controlled to fall in the range of ~30–100 nm.^[57] In many methods, Si/SiO₂ based nanomaterials such as silica nanoparticles are used to finely control film thickness and surface roughness due to their excellent optical property and the convenient further chemical treatment.^[60-64] Cohen *et al.* reported a layer-by-layer method to fabricate transparent superhydrophobic films with limited light scattering.^[62] SiO₂ nanoparticles

of various sizes are introduced into the multilayer thin film to adjust surface roughness. The obtained transparent superhydrophobic film is also antireflective, due to the low refractive index of the resultant porous multilayer films. Compared with inorganic films, polymer films of transparency and superhydrophobicity have their own advantages such as flexibility, controllable toughness and moduli.^[65,66] Kim *et al.* demonstrated a fabrication strategy using nanoimprint lithography with a flexible mold.^[66] A PDMS thin layer is coated on the mold to decrease surface energy of mold and used as an anti-adhesion layer coating for high-resolution nanoimprint lithography.

One of the important applications of antireflective superhydrophobic coatings is to increase the performance of solar cells. The nonwetting surface can prevent moisture and dirt accumulation and make the surface slippery and abrasion-resistant, which is potentially another way to increase the device efficiency.^[67] Recently, a kind of bio-inspired surface structure of self-cleaning property and broadband antireflectivity has been reported.^[68] Inspired from the antireflection structure of moths eyes^[69,70] and the self-cleaning ability of cicada wings,^[1-19] which consist of similar nonclose-packed arrays of nipples, Jiang P. *et al.* developed a simple and scalable reactive ion etching technique to make subwavelength antireflection coatings on silicon and glass substrates using wafer-scale production of nonclose-packed colloidal crystals as a template (**Figure 4**). The etched surface exhibits much lower reflection (<2.5%) over the whole spectrum, indicating broadband antireflection. After modified with fluorosilane, the surface can easily achieve superhydrophobicity with self-cleaning effect. This kind of surfaces is considered to have potential technological applications ranging from solar cells and photodiodes to flat panel displays and other optical components.

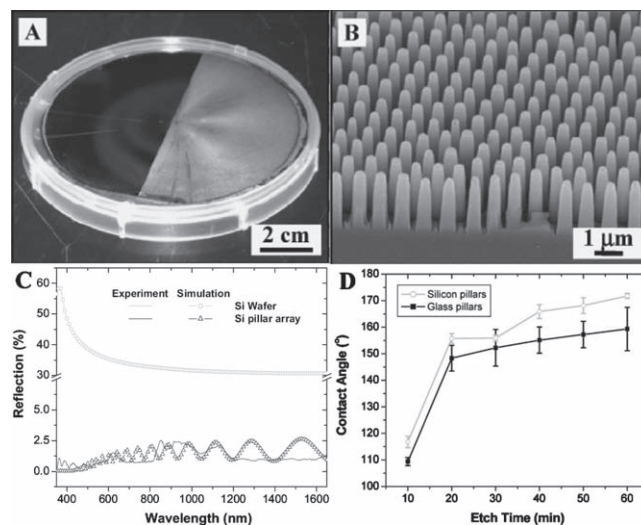


Figure 4. The bio-inspired self-cleaning antireflection silicon pillar arrays.^[68] (A) Photograph of a ~10 cm silicon wafer with the right half covered by subwavelength pillars and the left half unetched. (B) SEM image of silicon pillars after 50 min etching. (C) Experimental (solid) and imulated (dotted) specular reflection at normal incidence from a flat silicon wafer and a 60 min etched silicon pillar array. (D) Apparent water CA of templated silicon and glass pillar arrays at different etching durations. Reprinted with permission.^[68] Copyright 2008 Wiley-VCH.

2.4. Anti-Freezing and Anti-Snow

Adhesion of ice or wet snow to outdoor surfaces is well known to cause serious problems. However, almost no materials or surfaces currently can achieve completely repellence of ice or wet snow, because the liquid freezing will always happen when the temperature decreases to the freezing point. In addition to the extraordinary abilities of water-repellency and self-cleaning, superhydrophobic surface provides compatible approach in reduced ice adhesion or delayed freezing.^[71–81]

Kulinich *et al.* investigated the artificially created glaze ice strength (similar to accreted in nature) on flat hydrophobic and rough superhydrophobic coatings with similar self-assembled monolayers.^[78–80] Glaze ice is prepared by spraying supercooled water microdroplets on the target substrates at sub-zero temperature. Ice adhesion is evaluated by spinning the samples at constantly increasing speed until ice delamination occurred. They revealed that the previously reported^[73–75] direct correlation between ice repellency and contact angle on superhydrophobic surfaces was only valid for surfaces with low wetting hysteresis.^[79] By comparing with superhydrophobic surfaces of different contact angle hysteresis, they found that the contact angle hysteresis was another factor that influences the ice-solid adhesion strength.^[80] Quéré *et al.* demonstrated that freezing was significantly delayed when depositing water on cold superhydrophobic materials.^[81] The regular tap water is used in the experiments, which contains enough impurities to trigger freezing at 0 °C. It is observed that the presence of microtextures dramatically delay the freezing time of the water drops, by a factor between 3 and 5. Droplets roll off the superhydrophobic surface quickly without depositing any film and without freezing. Conversely, drops on flat copper spread more and ran slower, so that it leaves a film that freezes immediately. They pointed out that the air sublayer in a superhydrophobic surface could provide substantial thermal insulation and thus delayed the freezing process on cold superhydrophobic materials. These distinct results confirm the significant different in freezing kinetics between both kinds of substrates, which was helpful to illustrate that water repellency is an excellent strategy to avoid formation of ice on cold solids. Recently, Gao *et al.* fabricated a kind of nanoparticle-polymer composite superhydrophobic surfaces by mixing a hydrophobic polymer binder with silica particles ranging from 20 nm to 20 μm in diameter.^[77] They demonstrated the anti-icing capability of the prepared surfaces and reported the direct experimental evidence that such surfaces were able to prevent ice formation upon impact of supercooled water both in laboratory conditions and in natural environments (Figure 5). They found that the anti-icing capability of these composites depended not only on their superhydrophobicity but also on the size of the particles exposed on the surface. The authors attributed the observed dramatic increase of the icing probability to the continuously decrease of energy barrier as the result of the increase of particle size, for the icing probability was an exponential function of the free energy barrier.

Frost formation on a cold surface is another process that will cause energy waste and result in many negative effects on practical systems such as air conditioners, refrigerators, aircrafts, and so on. Frost formation on a cold surface involves two

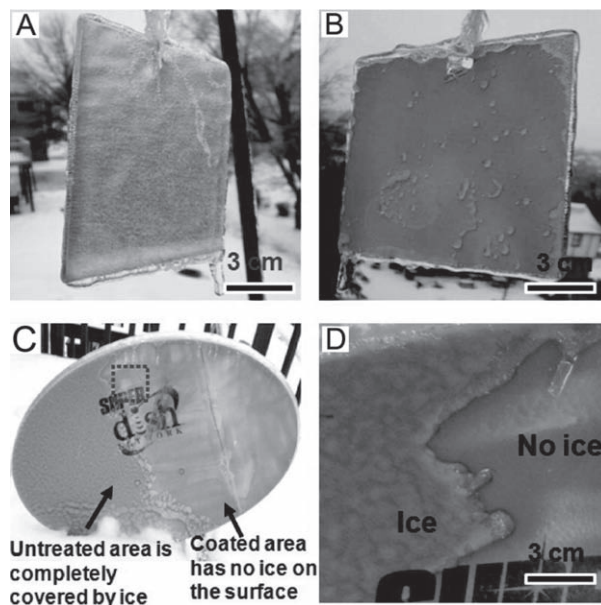


Figure 5. Test of anti-icing properties in naturally occurring “freezing rain”.^[77] (A) Untreated side and (B) treated side of an aluminum plate after the natural occurrence of “freezing rain”. (C) Satellite dish antenna after the freezing rain. (D) Close-up view of the area labeled by a red square in (C). Reprinted with permission.^[77] Copyright 2009 American Chemical Society.

distinct processes: nucleation and crystal growth. The nucleation process requires that water vapor must overcome a certain Gibbs energy barrier.^[82] Controlling the initial frost nucleation on cold surface will be helpful to delay or the process of frost formation. Na *et al.* gave a fundamental understanding of factors affecting frost nucleation, particularly the surface energy of the base surface.^[83] They found that air at the cold surface should be supersaturated to ensure frost nucleation. While the supersaturation degree is dependent on the surface energy, which will in return affect the initial frost nucleation. Their results showed that cold substrates of lower surface energy require higher supersaturation degree for nucleation than do higher energy surfaces, and surface roughness will also reduce the required supersaturation degree. As the extreme of low energy surface, superhydrophobic films are also considered as promising materials for alleviating frost growth on cold substrates. Liu *et al.* investigated the frost formation on a cold superhydrophobic copper surface under natural convection.^[84] On the superhydrophobic surface the frost formation is delayed and the frost layer exhibits a new structure that is similar to a cluster of chrysanthemum petals. Comparing with the frost layer structure formed on a plain copper surface, this kind of structure is weaker, looser, thin and easy to be removed. Recently, He *et al.* reported that superhydrophobic surface could great retard the frost formation process.^[85] The hydrophobic and superhydrophobic isotactic polypropylene (i-PP) films are fabricated to investigate their different effects on the process of frost formation. The frost formation is retarded on the prepared superhydrophobic surface, comparing with that on the flat hydrophobic surface. Moreover, the surface wettability of water increases steadily on the hydrophobic surface, but it oscillates

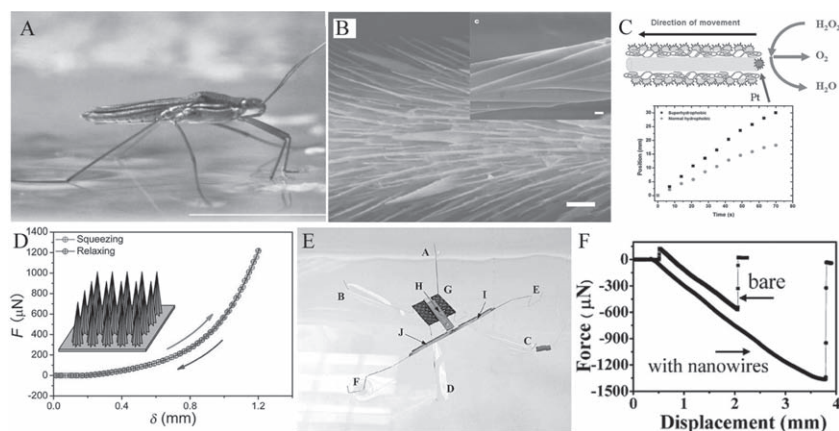


Figure 6. The superhydrophobic water strider legs. (A) Photograph of a water strider standing on the water surface.^[15] Reproduced with permission.^[15] Copyright 2003 Nature Publishing Group. (B) SEM image of the leg with oriented spindly setae and the nanogrooves on a single seta (inset in (B)).^[16] Reproduced with permission.^[16] Copyright 2004 Nature Publishing Group. (C) The position of the superhydrophobic and normal hydrophobic gold threads versus time of movement.^[86] Reproduced with permission.^[86] Copyright 2007 Wiley-VCH. (D) Bio-inspired model of ribbed nanoneedle array suggested for generating a robust superhydrophobicity.^[87] Reproduced with permission.^[87] Copyright 2010 Wiley-VCH. (E) The proposed robot mimicking water strider.^[88] Reproduced with permission.^[88] Copyright 2007 IEEE. (F) Comparison for the supporting force of the bare hydrophobic copper leg and the superhydrophobic copper leg.^[89] Reproduced with permission.^[89] Copyright 2010 Wiley-VCH.

on the superhydrophobic surface of micro- and nanometre structures, showing a kind of metastable three phase line (TPL). This metastable TCL will lead to the delay of the solidification at the TPL region, and retards the frost formation.

2.5. Bio-Inspired Aquatic Materials and Devices

Water striders (Figure 6a) are a kind of aquatic insects that can stand effortlessly, move and jump rapidly on water surfaces.^[15] Authors' group reported that the supporting legs of water strider are superhydrophobic, as the result of the combination of the hierarchical surface structure of needle-shaped setae with fine nanogrooves on them and the covered hydrophobic wax layer (Figure 6b).^[16] Besides the reported superior aquatic supporting force, the water strider legs are also considered to perform remarkable fluid drag reduction on aquatic surface. These can give inspirations for the applications in drag reducing materials and miniaturized aquatic devices.

Shi *et al.* reported that an artificial leg of superhydrophobic coating ($\sim 156^\circ$) can provide 0.4 mN supporting force per centimeter more than one of flat hydrophobic coating ($\sim 110^\circ$) as the result of the enhanced curvature force by superhydrophobic surface.^[90] By comparing the artificial hydrophobic and superhydrophobic legs, they also demonstrated that air trapped in the superhydrophobic coating can reduce the fluidic drag for objects moving on water.^[86] With the same propulsion, the velocity of a superhydrophobic gold thread is as much as 1.7 times that of a normal hydrophobic gold thread (Figure 6c). Su *et al.* reported the comparison of the movement of superhydrophobic and normal hydrophilic balls in water (using solid balls) or on water surface (using hollow balls). The superhydrophobic ball behaves a faster movement of floating on the water surface

than the normal glass ball, due to the reduction of skin friction owing to the increased area of the solid/air interface. In contrast, the relative slow movement of superhydrophobic ball under water shows that the dense microbubbles trapped at the solid/water interface around the superhydrophobic ball might act as an enhancer for the friction drag in water. Inspired from unique microstructure on water strider legs, Yao *et al.* designed and fabricated a water repellent material of ribbed, conical nanoneedle structure where oriented nanogrooves sculptured on the lateral nanoneedle surface (Figure 6d).^[87] Water droplets can perform a fully reversible exploration between the surfaces under the forced squeeze and relaxation. The proprietary lateral nanogrooves at the conical nanoneedles are considered to provide reliable contact lines for the easily depinning of the deformed interface when force is released. Besides the implication for the design of robust superhydrophobicity, this work gives a microscopic view of the reducing interface hysteresis of water-repellent materials.

For the aspect of bio-inspired superhydrophobic coatings of enhanced aquatic supporting force, attempts are performed to design and fabricate water-repellent materials and bio-inspired microscale aquatic device of high aquatic supporting force and water-walking ability.^[88,91-93] Sitti's group proposed a miniature robot of optimized support legs to mimic the water strider, and the developed robot could perform a linear motion of 3 cm/s without penetrate water surface (Figure 6e).^[88,91] Pan *et al.* fabricated a kind of miniature boats of high loading capacity by superhydrophobic copper meshes.^[93] Such a boat of 8.0 cm³ in volume can readily achieve a loading capacity greater than 11.0 g. Jiang *et al.* proposed superhydrophobic surfaces composed of crystalline nanowires of an organic semiconductor.^[89] After the model leg is coated with the superhydrophobic films, the maximal supporting force of the artificial leg' increases at least 2.4 times (Figure 6f). 1.0 mg of such organic crystalline nanowires assemble on the mimicked legs can maximally float a 372 mg model strider, indicating the striking water-repellent ability of the model leg. Potential application of such aquatic robot or device is thought to be useful in the areas such as environmental monitoring on lakes or rivers with wireless communication devices and biochemical sensors on board.

3. Application of Patterned Wettability

3.1. Water Collection

Efficient water collection from humid atmosphere is critical for biological livings in water-limited areas. One striking example is Namib desert *Stenocara* beetle, which uses the surface of patterned wettability on its back to collect drinking water from

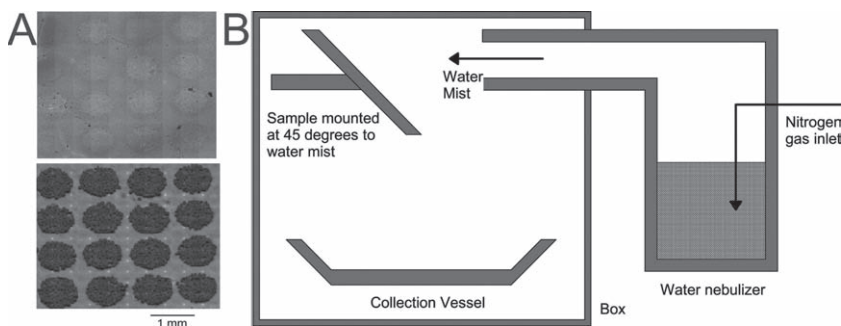


Figure 7. Hydrophobic surfaces with hydrophilic patterns and their water collection efficiency investigation.^[95] (A) Optical images of a typical hydrophobic surface with circular hydrophilic patterns. (B) Apparatus for water collection efficiency measurements. Reproduced with permission.^[95] Copyright 2007 American Chemical Society.

fog-laden wind.^[20] The beetle's back consists of alternating hydrophilic bumps and superhydrophobic channels. In a foggy dawn, the hydrophilic bumps can collect water from the atmosphere and the superhydrophobic channels can help to guide the accumulated water droplets to flow directly down to the beetle's mouth. Inspired by this surface design, Cohen *et al.* have fabricated hydrophilic or superhydrophilic patterns on superhydrophobic surfaces to mimic the function of the beetle's back via a polyelectrolytes alternate deposited technique.^[94] The wettability patterns exhibit extreme hydrophobic contrast. Water sprayed on superhydrophobic patterns will form spherical droplets. Most of the droplets bounce and roll on the superhydrophobic regions and eventually adhere to the hydrophilic patterns. As a demonstration of mimicked potential of the desert beetle, Badyal *et al.* reported their work of water collection on surfaces of series superhydrophobic/hydrophilic patterns.^[95] The water-collecting capabilities of different superhydrophilic spot size and pattern ratios are investigated in detail (Figure 7). Recently, Ruhe *et al.* fabricated series superhydrophobic surfaces that patterned with smooth circular hydrophilic domains, and investigated the influence of wettability contrast on the dewetting and rolling off behaviors of the collected drops.^[96] They found that the pinning force for a droplet on a given hydrophilic domain was constant and did not depend on the drop volume. These results indicate that the water collection efficiency could be optimized by controlling the wettability contrast of superhydrophobic/hydrophilic patterns as well as the ratio of the pattern areas.

3.2. Liquid Transportation

Droplets sitting on surfaces of different wetting state will present different contact areas, contact angles and contact angle hysteresis. Hence, it is possible to control droplet motion and liquid transportation by tuning surface wettability. In fact, liquid transportation is an active area for researchers. As the size effect and many dynamic factors must be considered for fluid transportation in microfluidics, here, we just discuss the liquid transportation in the open system, particularly on two dimensional surfaces, which might be roughly divided into two aspects, self-propelled motion and controllable liquid motion.

Brochard *et al.* reported the motions of droplets on solid surfaces induced by chemical or thermal gradients, in which the Marangoni effect plays an important roll.^[97] Whitesides *et al.* first reported the moving uphill of a water droplet on a surface of gradient wettability.^[98] The self-motion of the droplet is driven by the imbalanced forces due to the gradient surface tension acting on the solid-liquid contact lines of the droplet. Quere *et al.* reported the self-propelling behavior of wetting silicone oil drop on a conical fiber, in which the driving force is shown to be a gradient of Laplace pressure of the asymmetric droplets.^[99] Constructing specific surface roughness is also an efficient way to achieve droplets self-motion.^[100–102]

The surface roughness design can, on one hand, construct gradient wettability; and on the other hand, provide pathway and reduce energy barrier to guide droplet movement. When introducing stimuli-responsive gradient surface, movements of droplets can be guided by the external controls. Methods such as light-responsive,^[103–105] electrofield responsive,^[106] chemical driven^[107–109] or vibrations^[110,111] have been developed to achieve the smart control of droplet motions. Besides the wetting induced droplet motion and transportation, tuning the adhesion between droplet and substrate is also useful in controlling droplet mobility. Author's group has reported the no-lost transport of water microdroplet^[112] and superparamagnetic microdroplet^[113] using the superhydrophobic PS nanotube arrayed surface of high adhesive force. Besides, a kind of superhydrophobic iron surface that exhibits tunable adhesive force with the superparamagnetic microdroplet as a function of the magnetic field is also developed.^[114] These superhydrophobic surfaces indicate a kind of "mechanical hands" to grasp and transport water droplets.^[115]

One important application for the surfaces of droplet self-motion is to enhance heat transfer on solid surface. When humid steam passes over a colder hydrophobic substrate, water droplets will nucleate and condense on the substrate. To fast remove the condensed water droplets from the colder substrate will be appreciated in the heat transfer process of phase flow. Chaudhury *et al.* reported the fast movement of droplets on a wettability gradient surface from phase changes (Figure 8).^[116] It is found that, when a surface tension gradient is designed into the substrate surface, the merging droplets exhibits directional movements toward the more wettable side of the surface. Powered by the energies of coalescence and collimated by the forces along the wettability gradient, small drops (0.1 to 0.3 mm) present speeds of hundreds to thousands times faster than those in typical Marangoni flows. Such coalescence-induced drop motion is proposed to be useful to enhance the performance of heat exchangers by the authors. The proposed gradient surface design can effectively remove the insulating water from the surface of heat exchangers which usually weaken the heat transfer efficiency between the steam flow and the heat exchanger. In a designed experiment, the surface treatment enhances the heat transfer by a factor of 3 when the surface is subcooled from that of steam by about 20 °C and by

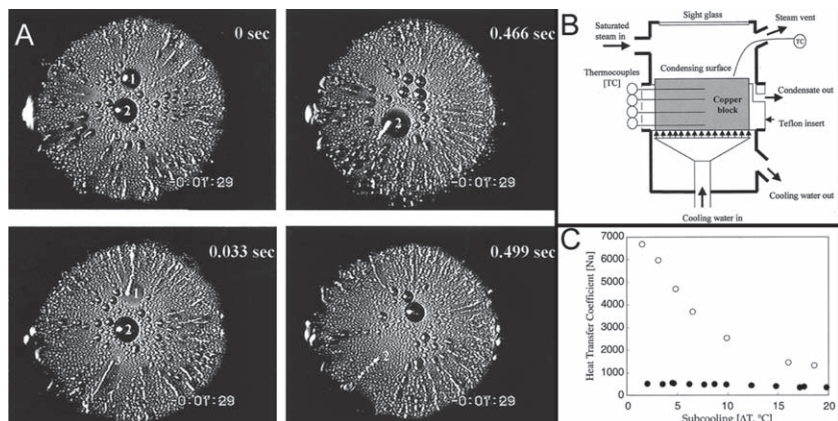


Figure 8. Enhanced heat transfer on the surface of gradient wettability.^[116] (A) Fast movements of condensed water drops resulting from the steam on a silicon wafer of a radial wettability gradient. (B) Schematics of a heat exchanger based on the surface of gradient wettability. (C) The comparison for the heat transfer coefficient on the surfaces of homogenous wettability (closed circle •) and gradient wettability (open circle ◦). Reprinted with permission.^[116] Copyright 2001 American Association for the Advancement of Science.

a factor of 10 when subcooling is about 2 °C. Moreover, the motion mechanism will be also valid in the situations of horizontal surfaces of heat exchangers and for those operating in microgravity situations, where the gravity-driven methods do not work.

3.3. Nanomaterial Positioning

In fabricating device, to locate functional micro- or nanomaterials in target position is as important as their properties. Among the common nanomaterials patterning methods, using wettability contrast patterns to position micro- or nanomaterials on 2D substrate has been demonstrated as a simple and convenient method.^[117–124] The key component for the patterning method is that the carrier phases can perform distinct wetting or dewetting behavior on the lyophilic/lyophobic patterned substrate to selectively locate the carrying materials. Whitesides *et al.* reported the fabrication of ordered 2D arrays of micro- and nanoparticles by using patterned self-assembled monolayers (SAMs) templates.^[117,118] Gold substrates were firstly modified with patterned grids of hydrophobic (CH₃-terminated) and hydrophilic (COOH-terminated) SAMs by microcontact printing. After immersing the patterned substrates in a calcium chloride solution and a following explosion to carbon dioxide, ordered crystallization of calcite can be achieved in the polar regions, where the rate of nucleation is fastest (Figure 9a).^[117] Similarly, inorganic salt crystal patterns can be obtained by immersing the substrate into solutions of CuSO₄ or KNO₃

and then withdrawn and dried.^[118] The solution wets and is retained exclusively on the hydrophilic regions of the surface, and the pattern properties such as size, shape, and liquid contact angle will fix the volume of liquid in each drop retained on the surface, forming ordered micro- or nanoparticles after the drops evaporation. Xia *et al.* used a similar method to pattern ordered magnetic nanoparticles on silicon substrates.^[119] Bao *et al.* demonstrated that both metallic nanorods^[121] and organic semiconducting single crystals^[122] could be assembled and aligned on surfaces with patterned wettability. The substrates are functionalized with different SAMs to achieve the desired wettability patterns and to control the solvent wetting and dewetting on desired pattern area. Solution with nanomaterials spreads on the substrate, dewets at the lyophobic patterns, accumulates and dries at the lyophilic patterns.

Gu *et al.* reported the fabrication of colloidal crystal films on specific areas of substrates that took advantage of the photocatalytic and photoinduced superhydrophilic properties of TiO₂ (Figure 9a).^[123] The prepared flat TiO₂ surface is firstly modified with fluoroalkylsilane SAM, to achieve surface hydrophobic with contact angle about 100°. The substrate is following irradiated with ultraviolet light through a photomask to make a wettability pattern with the contact angle of irradiated area to 0°, resulting in large wettability contrast.

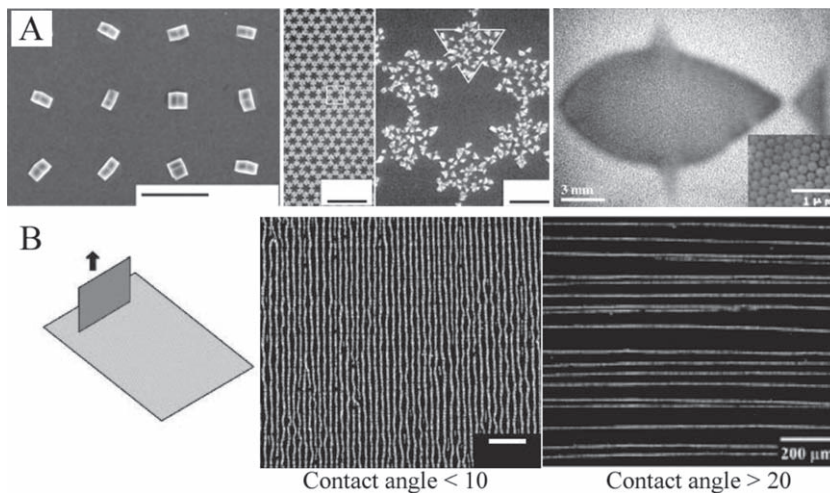


Figure 9. Nanomaterials positioning utilizing surface wettability. (A) Nanomaterials positioning on surfaces of patterned wettability. Left and middle: the patterned CaCO₃ crystals.^[117] Reprinted with permission.^[117] Copyright 1999 Nature Publishing Group. Right: The fish-shaped patterned colloidal crystals.^[123] Reproduced with permission.^[123] Copyright 2002 Wiley-VCH. The inset shows the arrangement of polystyrene spheres in the film. (B) Dip-coating nanomaterials patterning via dewetting LB monolayers. Left: the proposed illustration.^[125] Reprinted with permission.^[125] Copyright 2005 Nature Publishing Group. Optical microscopy images of the obtained nanoparticle stripe patterns on a completely wettable surface^[125] (middle) and a more hydrophobic surface^[126] (right). Reprinted with permission.^[125] Copyright 2006 American Chemical Society.

The substrate is then inserted vertically into an aqueous suspension containing either monodispersed silica spheres or polystyrene to fabricate a patterned colloidal crystal film. Colloidal crystals form over the hydrophilic areas during the lifting process, while no film is observed on the hydrophobic regions, due to the different capillary forces between the two areas. Recently, Javey *et al.* reported a generic positioning method of nanomaterials through a complementary design of carrier and stationary phases.^[124] The stationary substrate is modified as hydroxyl-terminated and fluoro-terminated regions. A water-soluble triblock copolymer, F-127 is used to encapsulate the nanomaterials. The encapsulation of F-127 polymer is a kind of non-covalent modification that can preserve the materials' intrinsic chemical and physical properties during the location and thus make the assembly independent of materials' intrinsic property. The hydroxyl groups on stationary substrate and on F-127 will take effective chemical interactions, and the polymer-encapsulated nanomaterials can be selectively anchored to the hydroxyl-modified regions during the solution dewetting process.

Utilizing the dewetting meniscus is also useful in directing nanomaterials, where the dispersed nanomaterials will assemble at the moving contact lines. Compared with the pre-defined template method, this kind of direct self-assembly method is highly desirable because of its simplicity and compatibility with heterogeneous integration processes. A simple example is to prepare vast colloidal crystals on solid substrate via the vertical deposition method, where the assembly at the meniscus is driven by the lateral capillary forces of the nanospheres. Yang's group reported a one-step dip-coating nanomaterials patterning method based on dewetting properties of Langmuir-Blodgett (LB) monolayers (Figure 9b).^[125–128] By controlling the dewetting and evaporation rate of the solution meniscus, nanoparticles or nanowires at the contact line are carried off the surface film and dried onto the substrate. When a completely wettable substrate (water contact angle $<10^\circ$) is used to be pulled vertically through a LB monolayer, ordered micrometer-scale stripes are deposited perpendicular to the meniscus.^[125] Stripe formation results from convective flows at the moving contact line of the colloidal LB monolayer, where nanoparticles at the contact line segregate into periodical domains during the meniscus dewetting due to the fingering instability of the drying front.^[129,130] However, when a more hydrophobic substrate (water contact angle $>20^\circ$) is used, patterns of single-particle lines oriented parallel to the meniscus will be produced.^[127] In this condition, contact line pinning occurs at the meniscus formed between the particle monolayer and the partially wettable substrate. The pinned meniscus is dragged and stretched during the dip-coating process, and it finally breaks and recedes to a new pinning site on the substrate, resulting in a kind of "stick-slip" motion. So nanoparticle lines are deposited during a "stick" event and the spacing is due to the "slip" of the meniscus, leading to deposition of one-dimensional arrays of nanoparticles. Moreover, this method also enables the selective positioning of nanowires onto prefabricated electrodes.^[126] This method provides a complementary tool for nanoscale patterning that no specialized equipment is necessary

4. Integrated Surfaces and Devices

4.1. Oil-Water Separation and Mass Oil Adsorption Materials

Superhydrophobic surfaces are usually superoleophilic, because the low-surface-energy chemicals on superhydrophobic surfaces usually have similar surface energies with the oil drops (hydrocarbon materials), and the surface roughness will enhance the oleophilicity, leading to superoleophilicity. One intrinsic application for surfaces integrated with both superhydrophobicity and superoleophilicity is to be used in oil-water separation. Feng *et al.* firstly reported such application.^[131] They coat polytetrafluoroethylene (PTFE), which is a hydrophobic (water contact angle about 100° – 110°) and moderate oleophilic (hexadecane contact angle about 50° – 60°) material, onto a stainless mesh via a spray-and-dry method. Microscopic images indicate that the prepared mesh surfaces exhibit a kind of micro/nanocomposite structure. Water droplet shows spherical shape on the surface, with contact angle 156.2° and sliding angle about 4° , indicating surface superhydrophobicity. While a diesel oil droplet could spread and permeate the mesh film thoroughly within only 240 ms, indicating superoleophilicity. Mixtures of diesel oil and water can be successfully separated using this mesh film (Figure 10a). Based on this strategy, kinds of industrial machines with the function of high efficient oil-water separation have been developed, which are now equipped on the sea ships (Figure 10b). The core component of the machine is just the filtration cell filled with functional nanomaterials. Impurities larger than $5\ \mu\text{m}$ will be eliminated and the oil content in the filtrate can be reduced to 30 ppm.

Another important potential application of superhydrophobic surfaces with superoleophilicity is the fast and mass

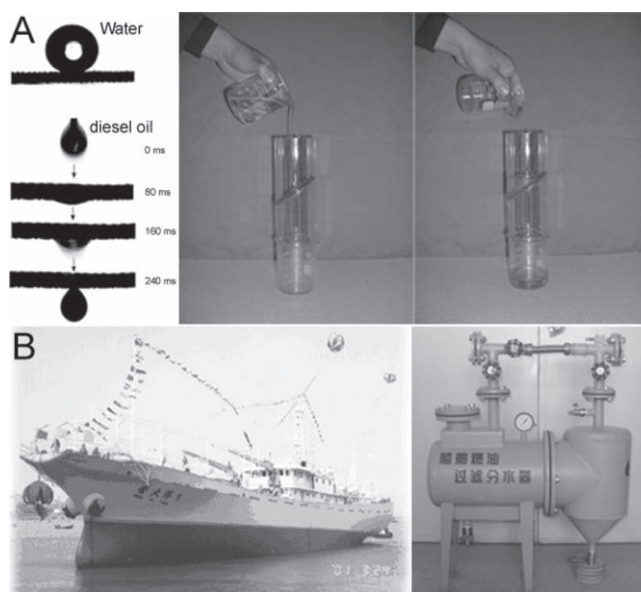


Figure 10. Oil-water separation using the films of superhydrophobicity and superoleophilicity.^[131] (A) A simple illustration of the oil-water separation by the prepared film. (B) The oil-water separation device used in ships. Reprinted with permission.^[131] Copyright 2004 Wiley-VCH.

oil adsorption. The design of suitable membranes for selective absorption of organics requires a material composed of superhydrophobic and oleophilic fibres that form a net of open superwetting capillaries. Stellacci *et al.* reported a kind of thermally stable free-standing superwetting nanowires membrane material.^[132] The membrane is based upon self-assembled, paper-like structures of cryptomelane-type manganese oxide nanowires. The unmodified nanowire membrane has a pore size distribution centered at 10 nm and a surface area of 44 m² g⁻¹. The wetting time for a water droplet (2 µL) adding to the surface is found to be 0.05 s, showing superhydrophilicity of fast water spreading and adsorption. The porous membrane will achieve superhydrophobic after modified with a hydrophobic thin layer, through heating a PDMS film and a following vapor deposition. This hydrophobic coating can be easily removed by heating the membrane to elevated temperatures (390 °C), resulting in switchable wetting behavior between superhydrophilic and superhydrophobic states. More importantly, the membrane combined its superwetting behavior (that is, superhydrophobicity) with good capillary action, an overall property called selective superabsorbance by the author. Specifically, the membrane absorbs on average 14 t m⁻³ of motor oil, making this membrane an ideal candidate as oil absorbent. And the membrane can selectively absorb emulsified oil suspensions in water with a remarkable uptake capacity of ~9 t m⁻³.

Recently, Cao and co-workers reported a carbon nanotube sponges of high structural flexibility and robustness, and wettability to organics in pristine form.^[133] The sponges are synthesized by chemical vapor deposition, in which nanotubes are self-assembled into a three-dimensionally interconnected framework, with a density close to the lightest aerogels, a porosity of >99%. The carbon nanotube sponges can be deformed into any shapes elastically and compressed to large-strains repeatedly in air or liquids without collapse. The sponges in densified state swell instantaneously upon contact with organic solvents. They can absorb a wide range of solvents and oils with excellent selectivity, recyclability, and absorption capacities up to 180 times their own weight, two orders of magnitude higher than activated carbon. The sponges are very light, porous and water-repellent, thus they can float on water surfaces and absorb large-area spreading oil films, suggesting promising environmental applications. A small densified pellet floating on water surface can quickly remove a spreading oil film with an area up to 800 times that of the sponge. A more immediate application for these membrane materials will be in the removal of hydrophobic/oleophilic contaminants from water (for example, sea water or industrial discharge). Given the global scale of severe water pollution arising from oil spills and industrial organic pollutants, this study may prove particularly useful in the design of recyclable absorbents with significant environmental impact.

4.2. Anti-Bioadhesion

Surface properties of materials, including composition, topography, charge, flexibility and wettability, are of great importance in biological applications. Although these factors usually work together to have a cooperation effect, surface wettability which usually acts as an integrated factor, is one of the most important

parameters affecting protein adsorption, platelet adhesion, and cell adhesion.^[134–141] For example, proteins are usually easier to be adsorbed on hydrophobic surface than on hydrophilic surface, as the result of strong hydrophobic-hydrophobic interactions between the hydrophobic functional groups of protein and substrates. While weak adsorptions will happen at hydrophilic surface where bound water at the surface will lead to repulsive forces to the hydrophobic functional group of protein.

The protein adsorption at the material surfaces has significant influence on cell behavior, which means that surface wettability can be used to control cell adhesion. However, research for the effects of surface wettability on bio-adhesion does not always present consistent results. For example, Lampin *et al.* observed the enhancement of cell (chick embryo vascular and corneal explants) adhesion potential in relation to the PMMA roughness and the corresponding enhanced hydrophobicity which favored the adsorption of adhesive proteins.^[135] While Zelzer *et al.* found that fibroblasts adhered and proliferated preferentially on a chemical gradient surface from hydrophobic (plasma polymerized hexane) to hydrophilic (plasma polymerized allylamine).^[142] Besides, Shiu *et al.* developed a multi-component protein-patterning technique based on a switchable superhydrophobic surface that can tune from superhydrophobic to superhydrophilic by electro-wetting. It is reported that the surfaces in the superhydrophobic state exhibited a protein resistance similar to that of PEG surfaces. However, when the same surfaces were converted to a wetted state under an electric field, they promoted the adsorption of protein molecules.^[143] Although the surface wettability is usually realized as an integrated phenomenon of surface properties and interfacial interactions, it is still valuable to understand and explore the behaviors of bio-molecules or bio-organisms through wettability control. The possible aspects for the effects of surface wettability include surface chemistry, topology, and perhaps also surface dynamics.

Platelet adhesion and activation on material surfaces may lead to blood coagulation and thrombosis, which relies on the blood-compatibility of bio-materials and decide the successful application of artificial organ implantations and other blood-contacting medical devices.^[142,144–146] Besides the methods of biological treatments^[147,148] and chemical modification,^[149,150] to control the surface morphology and wettability has been revealed as an efficient way to enhance blood-compatibility and thus obtain antiplatelet adhesion materials. Sun *et al.* fabricated a kind of blood-compatible nanostructured superhydrophobic surfaces by dip-coating fluorinated poly(carbonate urethane) onto aligned carbon nanotube films.^[141] Compared with the ordinary smooth film, the prepared films show excellent anti-adhesion ability in the *in vitro* platelet adhesion test. The films can largely decrease the platelet adhesion; while for the platelets that are occasionally attached on the films, further activation and subsequent deformation and spreading will be avoided. The special nanostructure and the superhydrophobicity derived from it are ascribed to play crucial roles in this blood compatibility effect. Chen *et al.* reported a kind of antiplatelet and thermal-responsive surface, based on poly(N-isopropylacrylamide) (PNIPAAm) grafted silicon nanowire arrays.^[148] The as-prepared surfaces show largely reduced platelet adhesion *in vitro* both below and above the lower critical solution temperature (LCST)

of PNIPAAm ($\sim 32^\circ\text{C}$), while a smooth PNIPAAm surface exhibits the anti-adhesion behavior only below the LCST. This is distinct from the common view, because the PNIPAAm film is hydrophobic above the LCST while hydrophilic below the LCST. Contact angle and adhesive force measurements on oil droplets (1,2-dichloroethane) are performed in water (that is, a water/oil/solid system) to reveal the implications. In the water system, the PNIPAAm coated nanostructured surface remains a underwater superoleophobicity, with the contact angle of oil droplet higher than 140° when the temperature is switched from 20 to 37°C again. Moreover, the surface shows a low adhesive force in the adhesive force measurements at the temperature 20 or 37°C . These results show that the nanostructured surface keeps a relatively high ratio of water content and plays a key role in largely reducing the adhesion of platelets; however, this effect does not exist on the smooth PNIPAAm surface.

Fan *et al.* reported a simple method to prepare a multiscale surface structure on polydimethylsiloxane (PDMS) slabs, which was constructed of interlaced submicrometer ridges and protrusions of several tens of nanometers.^[151] Four kinds of PDMS slabs of multiscale surface, nanostructured surface, submicrometer structured surface and smooth surface are selected to explore their platelet adhesion (Figure 11). To simulate the flow of *in vivo* circulation, the substrates are placed in flow chambers where a suspension of adenosine diphosphate (ADP) activated platelets passes across. Compared with the other three surfaces, the multiscale-structured surface can greatly reduce activated-platelet adhesion under flow conditions. Adhesion work of the prepared substrates is measured by *in situ* atomic force microscopy (AFM) measurements to investigate the adhesion behaviors of different surfaces. Results also indicate that the adhesive platelets on the submicrometer-ridge structure are fewer than those on the smooth surface and the surface with nanoprotusions. The submicrometer-ridge structure that matches well with the size of the platelets is probably more influential than nanoprotusions on antiplatelet adhesion, because high adhesion work means a large interactional force of the particle with

the surface. Statistical results clearly reveal that the multiscale surface has the lowest adhesion work of about $(0.01 \pm 0.01) \times 10^{-18} \text{ J}$, and the smooth surface value of $(17.38 \pm 8.38) \times 10^{-18} \text{ J}$ is the highest. The adhesion work of the nanostructured surface $((8.03 \pm 4.48) \times 10^{-18} \text{ J})$ is significantly higher than that of the submicrometer structured surface $((0.32 \pm 0.30) \times 10^{-18} \text{ J})$. Besides the low adhesion work, the multiscale structure might also greatly increase the fluid velocity of the boundary layer, which will decrease the collision frequency of platelets with the surface adhesion, thus resulting in remarkable antiplatelet adhesion.

Considering the diversity of bio-systems and the complex environments, more comparable work are needed to reveal the beneath mechanism of how wettability takes effect on bio-applications.

4.3. Liquid Painting and Reprography

To precisely control liquid pattern on solid surface is critical in liquid painting and reprography. During the process, surface wettability play an important roll in droplet spreading and infiltration, which dominate the resolution of the desired patterns.

Tian *et al.* reported an approach to precisely control patterned wettability transition for liquid reprography via a photoelectric cooperative wetting process on a superhydrophobic surface of nanorod arrays.^[152] The aligned-ZnO nanorod arrays are first grown perpendicularly onto glass substrates, which are following coated with titanil phthalocyanine (TiOPc) as a composite photoconductor layer and modified by perfluorosilane to improve the surface hydrophobicity. Electrowetting is then investigated on the as-prepared aligned composite nanorod-array (ACNA) surface. When the applied voltage is higher then the threshold value (about 7.5 V in this system), electrowetting will happen, and the contact angle decreases from the initial value of about 158° to the saturation value of about 35° . Moreover, because of the photoelectric cooperative effect of the ZnO

nanorod and TiOPc composite surface, the threshold voltage for the electrowetting will decrease when white light with an intensity of $\sim 400 \text{ mW cm}^{-2}$ is illuminated on the ACNA surface. Thus, it is possible to carry out the photoelectric cooperative anisotropic wetting. That is, at a selected applying voltage lower than the threshold voltage, liquid patterns could be controlled through patterned light illumination. The electrowetting will be activated only at the position where light illuminated, and liquid will spread along the nanorod arrays but be confined by the surrounding superhydrophobic areas, indicating a type of anisotropic wetting. Based on this strategy, the author successfully performed the liquid reprography process, and the wetting error of the reported system could be well controlled, rendering a compatible strategy for liquid reprography.

Offset printing is the most common system used for printing low and high-volume jobs,

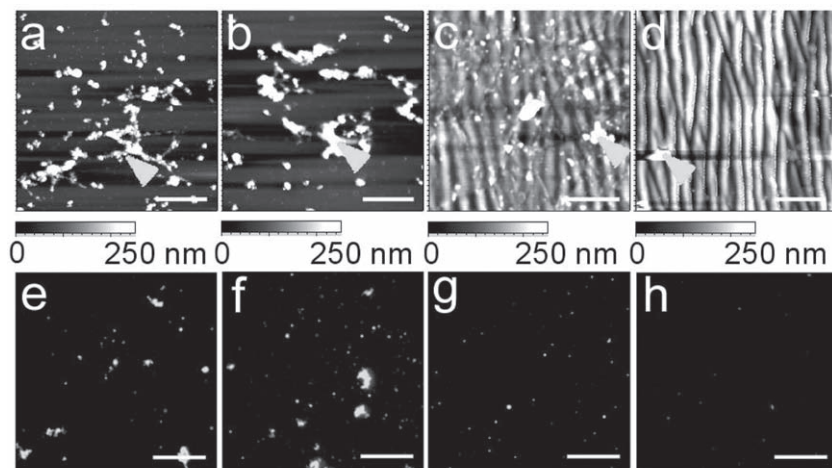


Figure 11. Platelet adhesion on the PDMS slabs of (A) smooth surface, (B) nanostructured surface, (C) submicrometer structured surface, and (D) multiscale surface.^[151] The upper images are the obtained AFM images, and the bottom images are the corresponding fluorescence images. Reprinted with permission.^[151] Copyright 2009 Wiley-VCH.

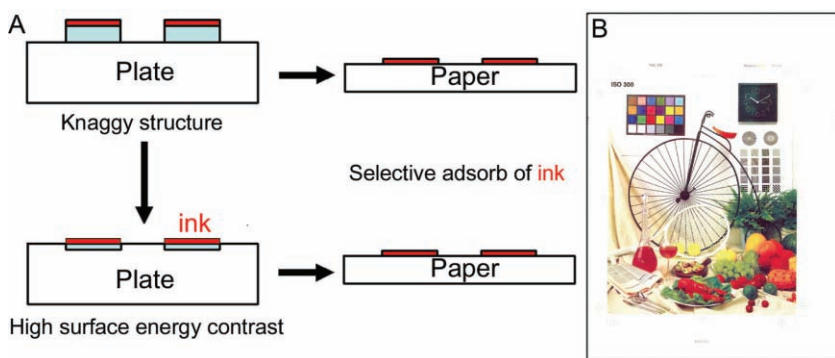


Figure 12. Direct inkjet computer-to-plate printing technique based on the high surface energy contrast patterns. A) The comparison of the traditional knaggy plate and the prepared printing plate in the offset printing process. B) The printed out colorful sample.

such as books and newspaper.^[153] In a typical process, the inked image on a printing plate is transferred to a rubber blanket, then to the printing paper or other surfaces (Figure 12a). The printing plates are usually made of metal, plastic, rubber and other materials, which are engraved or etched to form a knaggy pattern of the matter to be printed. The knaggy structures are used in the absorbance of the print ink and the final transferring print process. However, in the traditional plate making process, huge chemicals will be left in the fabrication and development of the knaggy plate, which will bring enormous waste and environmental pollution. Fujishima *et al.* reported serial works on the TiO₂ based superhydrophilic-superhydrophobic patterns for the application of off-set print.^[154,155] TiO₂ photocatalyst is firstly coating on fairly rough substrate following a surface modification with hydrophobic SAMs to achieve surface superhydrophobicity. The substrate is then patterned by an ink-jet method using aqueous UV light-resistant ink. The exposed SAM on the TiO₂ surface is decomposed by the full-area UV irradiation and thus becomes surface superhydrophilic. After the patterned aqueous ink is removed by water washing, superhydrophilic-superhydrophobic patterns can be prepared on the off-set printing plate. The as-prepared plate by this method is highly renewable. It's available for more than 5000-page prints, and a resolution of 133 LPI (line per inch) is also possible for color printing. The author's group has also developed a green nanotechnology of direct inkjet computer-to-plate printing technique. Figure 12b illustrates the mechanism of the printing process. The offset plates are made by directly inkjet printing imaging materials (functional nanomaterials dispersed in oleophilic ink solution) on the blank plate instead of the chemical or mechanical plate making process. By collaboratively tuning the surface energy of the imaging materials (oleophilic and hydrophobic) and the micro/nanostructure of the plate substrate (superhydrophilic), the spreading of the printed microdroplets (generally in picoliter volumes) can be well controlled due to the surface energy contrast of the ink solution and the plate substrate, and desired patterns can be obtained with fine resolution. Moreover, the printed patterns are superhydrophobic and oleophilic, while the non-printing area is still superhydrophilic and oleophobic, so the oil ink which is hydrophobic and oleophilic could selectively adsorb on the printed patterns, promising the high quality print on papers.

Using the printed plate, colorful images could also be obtained through overprinting (Figure 12c). Moreover, the obtained plate can be used for thousands of times, exhibiting good durability. Comparing with the traditional plate technique, the direct inkjet plate technique can efficiently decrease the waste of the plating materials and thus make the process economical and environmentally friendly.

4.4. Smart Microfluidics Devices

In microfluidic devices, microchannels and valves are characterized by a large surface-to-volume ratio, so that surface properties

strongly affect the flow behavior. Here, we give a brief look into the topic of how the surface wettability is introduced into the microfluidic devices and the extended applications of the integrated devices.

Superhydrophobic surfaces are considered to affect the fluid flows due to the formed air layer between the fluid and the solid surface and the established air/water boundary condition. Watanabe *et al.* reported a flow drag reduction phenomena when water passed through a 16-mm-diameter pipe with highly water repellent walls.^[156] The fluid slip is ascribed to the reduced molecular attraction and the resulted contact area between the water repellent walls and the liquid flow. Kim's experiments showed a dramatic reduction of liquid droplet flow resistance by the nanostructured superhydrophobic surfaces.^[157] Later Bizonne *et al.* confirmed the reduced friction effect of superhydrophobic surfaces with nanoscale roughness through numerical simulation.^[158] The slippage of the fluid at the channel boundaries was shown to be greatly increased by the nanopatterned surfaces. Joseph *et al.* measured the surface hydrodynamic properties of microchannels incorporated with superhydrophobic carbon nanotube forests.^[159] By tuning morphology of the surfaces, a no-slip boundary condition can be observed in the Wenzel state and slip lengths of a few microns in the Cassie superhydrophobic state. Moreover, the measured slip lengths are found to vary linearly with the lateral roughness scale L of carbon nanotube forests. Ou *et al.* reported the drop reductions of over 40% and apparent slip lengths exceeding 20 μm for the laminar flow of water through microchannels using hydrophobic surfaces with well-defined micron-sized surface roughness.^[160] The presence of the air-water interface and the resulting shear-free boundary condition results in the reduction. Choi *et al.* reported the slip effects on the superhydrophobic surface of nanoturf structures. Measured through a cone-and-plate rheometer system, a slip length of $\sim 20 \mu\text{m}$ for water flow and $\sim 50 \mu\text{m}$ for 30 wt% glycerin are observed.^[161] The essential geometrical characteristics of the conical nanoposts have been also analyzed.

Besides the drag reduction effect of superhydrophobic surfaces, recently, Steinberger *et al.* reported that gas trapped at a solid surface could also act as an anti-lubricant and promote high friction.^[162] They investigated the flow slippage on superhydrophobic channels with the surface embedded a

square lattice of calibrated cylindrical holes. Experimental and numerical results show that the presence of gas at the solid-liquid interface does not always reduce the friction. While the meniscus curvature at the holes is a key factor that has a dramatic influence on the boundary condition, and can turn it from slippery to sticky. The protruding menisci at the holes would result in a huge decrease of the effective slip length. And high protruding menisci, would also promote high friction, by trapping an immobile liquid layer of significant thickness above the solid wall. Based on their work, one can conclude that it is efficient way to integrate the control of menisci in fluidic microsystems designed to reduce wall friction. Recently, Hyv aluoma presented a two-phase lattice Boltzmann simulations of a Couette flow in a microchannel where one of the walls is hole-patterned and trapping with microbubbles.^[163] They provided a further observation of a decrease of a decrease of the slip with increasing shear rate which resulted in the bubble deformation. Considering the presented results, one can find that controlling slippage at the microchannels using superhydrophobic surfaces is still an open problem for surface engineering. The detailed effect of surface morphology should be taken into account rather than the simple factor of surface roughness.

The stability of the composite solid-air-liquid interface is very important to maintain the superhydrophobicity in the microchannel. Nanostructured surface design can be used to avoid the wetting state transition in the superhydrophobic microchannel.^[164] In the protein adsorption, the hydrophobic solid surfaces may adsorb proteins and the contact angle may change greatly. This is why the conventional capillary valve fails to hold/stop the protein solution. Based on the concept of superhydrophobicity, Lu *et al.* designed a kind of “fishbone” microvalve, which provided a robust valving function when dealing with protein blocking and protein solutions.^[165] The fishbone valve is able to stop the flow of 0.2 wt% BSA solution with food dye after protein blocking, and each microchannel of the fishbone provides a holding time of several hours. As a comparison, the traditional hydrophilic capillary valve can only maintain its function for both pure water and protein solution in the absence of protein blocking, but loses its function after protein blocking due to non-specific binding of proteins. This kind of valves can replace the capillary valve in applications where the chip surface requires protein blocking to prevent nonspecific binding.

Ionov *et al.* designed a kind of smart microfluidic channels by coating responsive mixed polymer brushes with a gradient of chemical composition on the walls of the channels.^[166] The surface wettability of the channel walls can be tuned between hydrophobic and hydrophilic, or a wetting gradient, by switching the behavior of the polymer brushes, which influences the interactions of the channel walls and the liquids in the channels, and brings new opportunities for manipulating the passage of liquids (Figure 13a,b). They firstly demonstrated the separation behavior for two immiscible liquids (water and toluene). A gradient mixed polystyrene (PS) and poly(2-vinylpyridine) brush (grad-PS-mix-P2VP) is firstly grafted on the Si wafer, which is then mounted on the T-shaped PDMS channel to assemble the microfluidic separation device. When exposed to acidic water (pH 2) and dried, the switching surface of grad-PS-mix-P2VP brush shows a lateral wetting gradient. The advancing water contact angle decreases gradually from 90° on the left-hand side

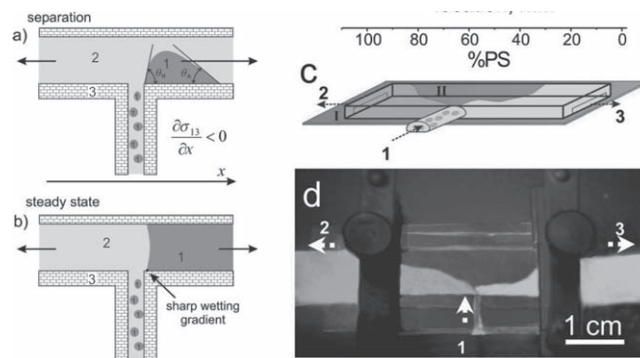


Figure 13. Smart microfluidics based on the switchable wettability of channel wall surface.^[166] Separation of immiscible liquids 1 and 2: Mechanism for (A) the drop formation when $\theta_R > \theta_A$, and (B) steady-state separation process. (C) The illustration and (D) the photograph of the fabricated device. Reprinted with permission.^[166] Copyright 2006 Wiley-VCH.

to 55° on the right-hand side of as the P2VP fraction increased, while the receding water contact angle decreases from 60° to 20°, respectively. After treatment with toluene, the gradient of advancing water contact angle is 95°–20°, and that of receding water contact angle is 74°–20°, respectively. In the reference experiments, the injected sample of water comes out from the right arm of the T-shaped junction, while the sample of toluene comes out from both the left and right sides equally, due to the different surface tension of the liquids. When a non-stabilized toluene–water emulsion is injected into the channel, it is spontaneously separated into two oppositely directed flows of liquids (Figure 13c,d). On one hand, water flows towards an increased fraction of P2VP in the mixed brush due to the strong gradient of the advancing and receding contact angles. And it becomes pinned due to a low value of the receding contact angle on the P2VP-rich area. On the other hand, toluene flows in the direction of the increasing PS fraction, resulting terms of the separation of the water-toluene emulsion. Moreover, the authors also presented selection, sensing, and dispensing of small volumes of liquids based on the concept of smart responsive channels. Combinations of these functional elements, complex microfluidic devices can be designed for analytical applications.

5. Summary and Outlook

In this review, recent progress of the applications of bio-inspired special wettability has been briefly summarized. Particular attention is devoted to applications of superhydrophobic surfaces, surfaces of patterned wettability, and multifunction devices based on special wettability. Although the field of bio-inspired special wettability has seen great progress, many problems still need to be resolved for industrial applications. First and foremost, researchers should be able to control the design of the surface with certain functionalities. Matching the material's structure and its function to the desired practical condition is of primary importance, which of course is sometimes a time-consuming process. We believe that learning from nature is an efficient way to shorten this process. Revealing nature's secret and further subtracting the beautiful mechanism can

render original inspirations, help to guide the research direction and bridge the gap between academic research and practical application. Secondly, the stability of the surface structure and functionality should be considered. The stability of the surface structure and functionality against external damage including mechanical stress and chemical contamination should be addressed as they can largely restrict the material's application. Thirdly, researchers should balance the cost of fabrication and the property and function of the materials. Most of present methods used to produce nanostructure surfaces are not compatible with large-scale fabrication with fast and low-cost processing. Thus, low-cost materials with a single-step fabrication strategy will be appreciated. Finally, the application of special wettable surfaces involves many fields, such as biology, physics, chemistry, material and engineering, and we believe that intensive collaboration of scientists from various disciplines is necessary to vigorously push the field forward, so as to bring great benefit to the society.

Acknowledgements

The authors thank the financial support by National Research Fund for Fundamental Key Projects (2010CB934700, 2009CB930404, 2007CB936403), and National Natural Science Foundation (20974113, 20601005). The Chinese Academy of Sciences is gratefully acknowledged.

Received: July 27, 2010

Revised: September 7, 2010

Published online: December 6, 2010

- [1] T. L. Sun, L. Feng, X. F. Gao, L. Jiang, *Acc. Chem. Res.* **2005**, *38*, 644.
- [2] F. Xia, L. Jiang, *Adv. Mater.* **2008**, *20*, 2842.
- [3] X. M. Li, D. Reinhoudt, M. Crego-Calama, *Chem. Soc. Rev.* **2007**, *36*, 1350.
- [4] X. Zhang, F. Shi, J. Niu, Y. G. Jiang, Z. Q. Wang, *J. Mater. Chem.* **2008**, *18*, 621.
- [5] D. Quéré, *Ann. Rev. Mater. Res.* **2008**, *38*, 71.
- [6] L. C. Gao, T. J. McCarthy, X. Zhang, *Langmuir* **2009**, *25*, 14100.
- [7] C. Dorner, J. Rühle, *Soft Matter* **2009**, *5*, 51.
- [8] X. J. Feng, L. Jiang, *Adv. Mater.* **2006**, *18*, 3063.
- [9] K. Koch, W. Barthlott, *Phil. Trans. Royal Soc. A – Math. Phys. Eng. Sci.* **2009**, *367*, 1487.
- [10] W. Barthlott, C. Neinhuis, *Planta* **1997**, *202*, 1.
- [11] C. Neinhuis, W. Barthlott, *Ann. Bot-London.* **1997**, *79*, 667.
- [12] L. Feng, S. H. Li, Y. S. Li, H. J. Li, L. J. Zhang, J. Zhai, Y. L. Song, B. Q. Liu, L. Jiang, D. B. Zhu, *Adv. Mater.* **2002**, *14*, 1857.
- [13] Y. M. Zheng, D. Han, J. Zhai, L. Jiang, *Appl. Phys. Lett.* **2008**, *92*, 084106.
- [14] P. P. Chen, L. Chen, D. Han, J. Zhai, Y. M. Zheng, L. Jiang, *Small* **2009**, *5*, 908.
- [15] D. L. Hu, B. Chan, J. W. M. Bush, *Nature* **2003**, *424*, 663.
- [16] X. F. Gao, L. Jiang, *Nature* **2004**, *432*, 36.
- [17] Y. M. Zheng, X. F. Gao, L. Jiang, *Soft Matter* **2007**, *3*, 178.
- [18] X. F. Gao, X. Yan, X. Yao, L. Xu, K. Zhang, J. H. Zhang, B. Yang, L. Jiang, *Adv. Mater.* **2007**, *19*, 2213.
- [19] W. Lee, M. K. Jin, W. C. Yoo, J. K. Lee, *Langmuir* **2004**, *20*, 7665.
- [20] A. R. Parker, C. R. Lawrence, *Nature* **2001**, *414*, 33.
- [21] Y. M. Zheng, H. Bai, Z. B. Huang, X. L. Tian, F. Q. Nie, Y. Zhao, J. Zhai, L. Jiang, *Nature* **2010**, *463*, 640.
- [22] M. J. Liu, S. T. Wang, Z. X. Wei, Y. L. Song, L. Jiang, *Adv. Mater.* **2009**, *21*, 665.
- [23] N. J. Shirtcliffe, G. McHale, M. I. Newton, C. C. Perry, F. B. Pyatt, *Appl. Phys. Lett.* **2006**, *89*, 104106.
- [24] G. Mchale, M. I. Newton, N. J. Shirtcliffe, *Soft Matter* **2010**, *6*, 714.
- [25] H. A. Schuyten, J. D. Reid, J. W. Weaver, J. G. Frick, *Text. Res. J.* **1948**, *18*, 396.
- [26] H. A. Schuyten, J. D. Reid, J. W. Weaver, J. G. Frick, *Text. Res. J.* **1948**, *18*, 490.
- [27] R. N. Wenzel, *Ind. Eng. Chem.* **1936**, *28*, 7.
- [28] A. B. D. Cassie, S. Baxter, *Trans. Faraday Soc.* **1944**, *40*, 546.
- [29] J. Vince, B. Orel, A. Vilčnik, M. Fir, A. S. Vuk, V. Jovanovski, B. Simončič, *Langmuir* **2006**, *22*, 6489.
- [30] M. Yu, G. T. Gu, W. D. Meng, F. L. Qing, *Appl. Surf. Sci.* **2007**, *253*, 3669.
- [31] T. Bahners, T. Textor, K. Opwis, E. Schollmeyer, *J. Adhes. Sci. Technol.* **2008**, *22*, 285.
- [32] L. C. Gao, T. J. McCarthy, *Langmuir* **2006**, *22*, 5998.
- [33] H. F. Hoefnagels, D. Wu, G. de With, W. Ming, *Langmuir* **2007**, *23*, 13158.
- [34] B. X. Leng, Z. Z. Shao, G. de With, W. H. Ming, *Langmuir* **2009**, *25*, 2456.
- [35] B. Tomšič, B. Simončič, B. Orel, L. Černe, P. F. Tavčer, M. Zorko, I. Jerman, A. Vilčnik, J. Kovač, *J. Sol-Gel. Sci. Techn.* **2008**, *47*, 44.
- [36] A. Vilčnik, I. Jerman, A. S. Vuk, M. Koželj, B. Orel, B. Tomšič, B. Simončič, J. Kovač, *Langmuir* **2009**, *25*, 5869.
- [37] J. Y. Kang, M. Sarmadi, *AATCC Rev.* **2004**, *4*, 29.
- [38] R. Morent, N. De Geyter, J. Verschuren, K. De Clerck, P. Kiekens, C. Leys, *Surf. Coat. Technol.* **2008**, *202*, 3427.
- [39] M. J. Tsafack, J. Levalois-Grutzmacher, *Surf. Coat. Technol.* **2007**, *201*, 5789.
- [40] J. Zhang, P. France, A. Radomyselskiy, S. Datta, J. A. Zhao, W. van Ooij, *J. Appl. Polym. Sci.* **2003**, *88*, 1473.
- [41] Editorial, *Nat. Mater.* **2005**, *4*, 355.
- [42] T. Kawai, H. Nishihara, K. Aramaki, *J. Electrochem. Soc.* **1996**, *143*, 3866.
- [43] F. P. Zamborini, R. M. Crooks, *Langmuir* **1998**, *14*, 3279.
- [44] F. Sinapi, L. Forget, J. Delhalle, Z. Mekhalif, *Appl. Surf. Sci.* **2003**, *212*, 464.
- [45] P. E. Hintze, L. M. Calle, *Electrochim. Acta* **2006**, *51*, 1761.
- [46] S. T. Wang, L. Feng, L. Jiang, *Adv. Mater.* **2006**, *18*, 767.
- [47] Z. G. Guo, W. M. Liu, B. L. Su, *Appl. Phys. Lett.* **2008**, *92*, 063104.
- [48] Z. B. Huang, Y. Zhu, J. H. Zhang, G. F. Yin, *J. Phys. Chem. C* **2007**, *111*, 6821.
- [49] H. Q. Liu, S. Szunerits, W. G. Xu, R. Boukherroub, *ACS Appl. Mater. Interfaces* **2009**, *1*, 1150.
- [50] E. Hermelin, J. Petitjean, J. C. Lacroix, K. I. Chane-Ching, J. Tanguy, P. C. Lacaze, *Chem. Mater.* **2008**, *20*, 4447.
- [51] F. Z. Zhang, L. L. Zhao, H. Y. Chen, S. L. Xu, D. G. Evans, X. Duan, *Angew. Chem. Int. Ed.* **2008**, *47*, 2466.
- [52] T. Liu, S. G. Chen, S. Cheng, J. T. Tian, X. T. Chang, Y. S. Yin, *Electrochim. Acta* **2007**, *52*, 8003.
- [53] T. Liu, Y. S. Yin, S. G. Chen, X. T. Chang, S. Cheng, *Electrochim. Acta* **2007**, *52*, 3709.
- [54] H. F. Meng, S. T. Wang, J. M. Xi, Z. Y. Tang, L. Jiang, *J. Phys. Chem. C* **2008**, *112*, 11454.
- [55] J. M. Xi, L. Feng, L. Jiang, *Appl. Phys. Lett.* **2008**, *92*, 053102.
- [56] W. C. Wu, X. L. Wang, D. A. Wang, M. Chen, F. Zhou, W. M. Liu, Q. J. Xue, *Chem. Commun.* **2009**, 1043.
- [57] A. Nakajima, A. Fujishima, K. Hashimoto, T. Watanabe, *Adv. Mater.* **1999**, *11*, 1365.
- [58] A. Nakajima, K. Abe, K. Hashimoto, T. Watanabe, *Thin Solid Films* **2000**, *376*, 140.
- [59] A. Nakajima, K. Hashimoto, T. Watanabe, K. Takai, G. Yamauchi, A. Fujishima, *Langmuir* **2000**, *16*, 7044.

- [60] Z. Z. Gu, H. Uetsuka, K. Takahashi, R. Nakajima, H. Onishi, A. Fujishima, O. Sato, *Angew. Chem. Int. Ed.* **2003**, *42*, 894.
- [61] G. R. J. Artus, S. Jung, J. Zimmermann, H. P. Gautschi, K. Marquardt, S. Seeger, *Adv. Mater.* **2006**, *18*, 2758.
- [62] J. Bravo, L. Zhai, Z. Z. Wu, R. E. Cohen, M. F. Rubner, *Langmuir* **2007**, *23*, 7293.
- [63] Y. Li, F. Liu, J. Q. Sun, *Chem. Commun.* **2009**, 2730.
- [64] M. Manca, A. Cannavale, L. De Marco, A. S. Arico, R. Cingolani, G. Gigli, *Langmuir* **2009**, *25*, 6357.
- [65] H. Yabu, M. Shimomura, *Chem. Mater.* **2005**, *17*, 5231.
- [66] M. Kim, K. Kim, N. Y. Lee, K. Shin, Y. S. Kim, *Chem. Commun.* **2007**, 2237.
- [67] B. G. Prevo, E. W. Hon, O. D. Velev, *J. Mater. Chem.* **2007**, *17*, 791.
- [68] W. L. Min, B. Jiang, P. Jiang, *Adv. Mater.* **2008**, *20*, 3914.
- [69] M. Srinivasarao, *Chem. Rev.* **1999**, *99*, 1935.
- [70] P. Vukusic, J. R. Sambles, *Nature* **2003**, *424*, 852.
- [71] H. Saito, K. Takai, H. Takazawa, G. Yamauchi, *Mater. Sci. Res. Int.* **1997**, *3*, 216.
- [72] H. Saito, K. Takai, G. Yamauchi, *Mater. Sci. Res. Int.* **1997**, *3*, 185.
- [73] H. Saito, K. Takai, G. Yamauchi, *JOCCA – Surf. Coat. Int.* **1997**, *80*, 168.
- [74] G. Yamauchi, K. Takai, H. Saito, *IEICE. T. Electron.* **2000**, *E83c*, 1139.
- [75] V. F. Petrenko, S. Peng, *Can. J. Phys.* **2003**, *81*, 387.
- [76] S. Suzuki, A. Nakajima, N. Yoshida, M. Sakai, A. Hashimoto, Y. Kameshima, K. Okada, *Chem. Phys. Lett.* **2007**, *445*, 37.
- [77] L. L. Cao, A. K. Jones, V. K. Sikka, J. Z. Wu, D. Gao, *Langmuir* **2009**, *25*, 12444.
- [78] S. A. Kulinich, M. Farzaneh, *Appl. Surf. Sci.* **2004**, *230*, 232.
- [79] S. A. Kulinich, M. Farzaneh, *Langmuir* **2009**, *25*, 8854.
- [80] S. A. Kulinich, M. Farzaneh, *Appl. Surf. Sci.* **2009**, *255*, 8153.
- [81] P. Tourkine, M. Le Merrier, D. Quéré, *Langmuir* **2009**, *25*, 7214.
- [82] N. H. Fletcher, *The Chemical Physics of Ice*, Cambridge, University Press, Cambridge, **1970**.
- [83] B. Na, R. L. Webb, *Int. J. Heat Mass. Tran.* **2003**, *46*, 3797.
- [84] Z. L. Liu, Y. J. Gou, J. T. Wang, S. Y. Cheng, *Int. J. Heat Mass. Tran.* **2008**, *51*, 5975.
- [85] M. He, J. X. Wang, H. L. Li, X. L. Jin, J. J. Wang, B. Q. Liu, Y. L. Song, *Soft Matter* **2010**, *6*, 2396.
- [90] F. Shi, Z. Q. Wang, X. Zhang, *Adv. Mater.* **2005**, *17*, 1005.
- [86] F. Shi, J. Niu, J. L. Liu, F. Liu, Z. Q. Wang, X. Q. Feng, X. Zhang, *Adv. Mater.* **2007**, *19*, 2257.
- [87] X. Yao, Q. W. Chen, L. Xu, Q. K. Li, Y. L. Song, X. F. Gao, D. Quéré, L. Jiang, *Adv. Funct. Mater.* **2010**, *20*, 656.
- [91] Y. S. Song, S. H. Suhr, M. Sitti, *IEEE International Conference on Robotics and Automation (Icra)* **2006**, Vols. 1–10, 2303.
- [88] Y. S. Song, M. Sitti, *IEEE Transactions on Robotics* **2007**, *23*, 578.
- [92] B. Shin, H. Y. Kim, K. J. Cho, *IEEE Ras & Embs International Conference on Biomedical Robotics and Biomechanics (Biorob 2008)* **2008**, Vols. 1 and 2, 127.
- [93] Q. M. Pan, M. Wang, *ACS Appl. Mater. Interfaces* **2009**, *1*, 420.
- [89] L. Jiang, X. Yao, H. X. Li, Y. Y. Fu, L. Chen, Q. Meng, W. P. Hu, L. Jiang, *Adv. Mater.* **2010**, *22*, 376.
- [94] L. Zhai, M. C. Berg, F. C. Cebecci, Y. Kim, J. M. Milwid, M. F. Rubner, R. E. Cohen, *Nano Lett.* **2006**, *6*, 1213.
- [95] R. P. Garrod, L. G. Harris, W. C. E. Schofield, J. McGettrick, L. J. Ward, D. O. H. Teare, J. P. S. Badyal, *Langmuir* **2007**, *23*, 689.
- [96] C. Dorrer, J. Ruhe, *Adv. Mater.* **2008**, *20*, 159.
- [97] F. Brochard, *Langmuir* **1989**, *5*, 432.
- [98] M. K. Chaudhury, G. M. Whitesides, *Science* **1992**, *256*, 1539.
- [99] E. Lorenceau, D. Quéré, *J. Fluid. Mech.* **2004**, *510*, 29.
- [100] J. L. Zhang, Y. C. Han, *Langmuir* **2007**, *23*, 6136.
- [101] J. L. Zhang, Y. C. Han, *Langmuir* **2009**, *25*, 14195.
- [102] N. Moradi, F. Varnik, I. Steinbach, *Europhys. Lett.* **2010**, *89*.
- [103] K. Ichimura, S. K. Oh, M. Nakagawa, *Science* **2000**, *288*, 1624.
- [104] S. K. Oh, M. Nakagawa, K. Ichimura, *J. Mater. Chem.* **2002**, *12*, 2262.
- [105] D. Yang, M. Piech, N. S. Bell, D. Gust, S. Vail, A. A. Garcia, J. Schneider, C. D. Park, M. A. Hayes, S. T. Picraux, *Langmuir* **2007**, *23*, 10864.
- [106] B. S. Gallardo, V. K. Gupta, F. D. Eagerton, L. I. Jong, V. S. Craig, R. R. Shah, N. L. Abbott, *Science* **1999**, *283*, 57.
- [107] U. Thiele, K. John, M. Bar, *Phys. Rev. Lett.* **2004**, *93*.
- [108] K. John, M. Bar, U. Thiele, *Eur. Phys. J. E* **2005**, *18*, 183.
- [109] S. W. Lee, P. E. Laibinis, *J. Am. Chem. Soc.* **2000**, *122*, 5395.
- [110] S. Daniel, M. K. Chaudhury, *Langmuir* **2002**, *18*, 3404.
- [111] S. Daniel, S. Sircar, J. Gliem, M. K. Chaudhury, *Langmuir* **2004**, *20*, 4085.
- [112] M. H. Jin, X. J. Feng, L. Feng, T. L. Sun, J. Zhai, T. J. Li, L. Jiang, *Adv. Mater.* **2005**, *17*, 1977.
- [113] X. Hong, X. F. Gao, L. Jiang, *J. Am. Chem. Soc.* **2007**, *129*, 1478.
- [114] Z. J. Cheng, L. Feng, L. Jiang, *Adv. Funct. Mater.* **2008**, *18*, 3219.
- [115] X. Y. Song, J. Zhai, Y. L. Wang, L. Jiang, *J. Phys. Chem. B* **2005**, *109*, 4048.
- [116] S. Daniel, M. K. Chaudhury, J. C. Chen, *Science* **2001**, *291*, 633.
- [117] J. Aizenberg, A. J. Black, G. M. Whitesides, *Nature* **1999**, *398*, 495.
- [118] D. Qin, Y. N. Xia, B. Xu, H. Yang, C. Zhu, G. M. Whitesides, *Adv. Mater.* **1999**, *11*, 1433.
- [119] Z. Y. Zhong, B. Gates, Y. N. Xia, D. Qin, *Langmuir* **2000**, *16*, 10369.
- [120] H. Liu, J. Zhai, L. Jiang, *Soft Matter* **2006**, *2*, 811.
- [121] S. H. Liu, J. B. H. Tok, J. Locklin, Z. N. Bao, *Small* **2006**, *2*, 1448.
- [122] S. H. Liu, W. C. M. Wang, S. C. B. Mannsfeld, J. Locklin, P. Erk, M. Gomez, F. Richter, Z. N. Bao, *Langmuir* **2007**, *23*, 7428.
- [123] Z. Z. Gu, A. Fujishima, O. Sato, *Angew. Chem. Int. Ed.* **2002**, *41*, 2068.
- [124] R. Yerushalmi, J. C. Ho, Z. A. Jacobson, A. Javey, *Nano Lett.* **2007**, *7*, 2764.
- [125] J. X. Huang, F. Kim, A. R. Tao, S. Connor, P. D. Yang, *Nat. Mater.* **2005**, *4*, 896.
- [127] J. X. Huang, A. R. Tao, S. Connor, R. R. He, P. D. Yang, *Nano Lett.* **2006**, *6*, 524.
- [126] J. X. Huang, R. Fan, S. Connor, P. D. Yang, *Angew. Chem., Int. Ed.* **2007**, *46*, 2414.
- [128] A. R. Tao, J. X. Huang, P. D. Yang, *Acc. Chem. Res.* **2008**, *41*, 1662.
- [129] A. M. Cazabat, F. Heslot, S. M. Troian, P. Carles, *Nature* **1990**, *346*, 824.
- [130] E. Pauliac-Vaujour, A. Stannard, C. P. Martin, M. O. Blunt, I. Nottingher, P. J. Moriarty, I. Vancea, U. Thiele, *Phys. Rev. Lett.* **2008**, *100*, 176102.
- [131] L. Feng, Z. Y. Zhang, Z. H. Mai, Y. M. Ma, B. Q. Liu, L. Jiang, D. B. Zhu, *Angew. Chem. Int. Ed.* **2004**, *43*, 2012.
- [132] J. K. Yuan, X. G. Liu, O. Akbulut, J. Q. Hu, S. L. Suib, J. Kong, F. Stellacci, *Nat. Nanotechnol.* **2008**, *3*, 332.
- [133] X. C. Gui, J. Q. Wei, K. L. Wang, A. Y. Cao, H. W. Zhu, Y. Jia, Q. K. Shu, D. H. Wu, *Adv. Mater.* **2010**, *22*, 617.
- [134] K. L. Prime, G. M. Whitesides, *J. Am. Chem. Soc.* **1993**, *115*, 10714.
- [135] M. Lampin, R. Warocquier-Clerout, C. Legris, M. Degrange, M. F. Sigot-Luizard, *J. Biomed. Mater. Res.* **1997**, *36*, 99.
- [136] J. H. Lee, H. B. Lee, *J. Biomed. Mater. Res.* **1998**, *41*, 304.
- [137] H. Elwing, *Biomaterials*, **1998**, *19*, 397.
- [138] N. Fauchaux, R. Schweiss, K. Lutzow, C. Werner, T. Groth, *Biomaterials* **2004**, *25*, 2721.
- [139] A. Sethuraman, M. Han, R. S. Kane, G. Belfort, *Langmuir* **2004**, *20*, 7779.
- [140] S. F. Chen, J. Zheng, L. Y. Li, S. Y. Jiang, *J. Am. Chem. Soc.* **2005**, *127*, 14473.
- [141] T. L. Sun, H. Tan, D. Han, Q. Fu, L. Jiang, *Small* **2005**, *1*, 959.
- [142] M. Zelzer, R. Majani, J. W. Bradley, F. R. A. J. Rose, M. C. Davies, M. R. Alexander, *Biomaterials*, **2008**, *29*, 172.
- [143] J. Y. Shiu, P. Chen, *Adv. Funct. Mater.* **2007**, *17*, 2680.

- [144] *Implantation biology: the host response and biomedical devices* (Ed: R. S. Greco), CRC Press, Boca Raton: **1994**.
- [145] N. A. Peppas, R. Langer, *Science* **1994**, *263*, 1715.
- [146] R. Langer, D. A. Tirrell, *Nature* **2004**, *428*, 487.
- [147] N. Maalej, R. Albrecht, J. Loscalzo, J. D. Folts, *J. Am. Coll. Cardiol.* **1999**, *33*, 1408.
- [148] L. Chen, M. J. Liu, H. Bai, P. P. Chen, F. Xia, D. Han, L. Jiang, *J. Am. Chem. Soc.* **2009**, *131*, 10467.
- [149] B. Balakrishnan, D. S. Kumar, Y. Yoshida, A. Jayakrishnan, *Biomaterials* **2005**, *26*, 3495.
- [150] K. Kaladhar, C. P. Sharma, *Langmuir* **2004**, *20*, 11115.
- [151] H. L. Fan, P. P. Chen, R. M. Qi, J. Zhai, J. X. Wang, L. Chen, L. Chen, Q. M. Sun, Y. L. Song, D. Han, L. Jiang, *Small* **2009**, *5*, 2144.
- [152] D. L. Tian, Q. W. Chen, F. Q. Nie, J. J. Xu, Y. L. Song, L. Jiang, *Adv. Mater.* **2009**, *21*, 3744.
- [153] *Handbook of Print Media: Technologies and Production Methods* (Ed: H. Kipphan), Springer-Verlag Berlin Heidelberg, New York **2001**.
- [154] S. Nishimoto, A. Kubo, K. Nohara, X. Zhang, N. Taneichi, T. Okui, Z. Liu, K. Nakata, H. Sakai, T. Murakami, M. Abe, T. Komine, A. Fujishima, *Appl. Surf. Sci.* **2009**, *255*, 6221.
- [155] K. Nakata, S. Nishimoto, A. Kubo, D. Tryk, T. Ochiai, T. Murakami, A. Fujishima, *Chem. Asian J.* **2009**, *4*, 984.
- [156] K. Watanabe, Yanuar, H. Udagawa, *J. Fluid. Mech.* **1999**, *381*, 225.
- [157] J. W. Kim, C. J. Kim, *Fifteenth IEEE International Conference on Micro Electro Mechanical Systems, Technical Digest* **2002**, 479.
- [158] C. Cottin-Bizonne, J. L. Barrat, L. Bocquet, E. Charlaix, *Nat. Mater.* **2003**, *2*, 237.
- [159] P. Joseph, C. Cottin-Bizonne, J. M. Benoît, C. Ybert, C. Journet, P. Tabeling, L. Bocquet, *Phys. Rev. Lett.* **2006**, *97*, 156104 1.
- [160] J. Ou, B. Perot, J. P. Rothstein, *Phys. Fluids* **2004**, *16*, 4635.
- [161] C. H. Choi, C. J. Kim, *Phys. Rev. Lett.* **2006**, 96.
- [162] A. Steinberger, C. Cottin-Bizonne, P. Kleimann, E. Charlaix, *Nat. Mater.* **2007**, *6*, 665.
- [163] J. Hyvaluoma, J. Harting, *Phys. Rev. Lett.* **2008**, 100.
- [164] D. Byun, J. Kim, H. S. Ko, H. C. Park, *Phys. Fluids* **2008**, 20.
- [165] C. M. Lu, Y. B. Xie, Y. Yang, M. M. C. Cheng, C. G. Koh, Y. L. Bai, L. J. Lee, *Anal. Chem.* **2007**, *79*, 994.
- [166] L. Ionov, N. Houbenov, A. Sidorenko, M. Stamm, S. Minko, *Adv. Funct. Mater.* **2006**, *16*, 1153.